

Supplementary Materials for
Neuronal activity drives FMRP- and HSPG-dependent matrix metalloproteinase function required for rapid synaptogenesis

Mary L. Dear, Jarrod Shilts, Kendal Broadie*

*Corresponding author. Email: kendal.broadie@vanderbilt.edu

Published 7 November 2017, *Sci. Signal.* **10**, eaan3181 (2017)
DOI: 10.1126/scisignal.aan3181

This PDF file includes:

- Fig. S1. Temperature controls for dTRPA1 activity-induced synaptic bouton formation.
- Fig. S2. Mmp2 is not required for activity-dependent synaptic bouton formation.
- Fig. S3. Mmp1 is rapidly and specifically increased after dTRPA1 neuronal stimulation.
- Fig. S4. Synaptic Mmp2 is rapidly reduced after acute neuronal stimulation.
- Fig. S5. Synaptic Dlp is rapidly increased after acute neuronal stimulation.
- Fig. S6. Synaptic Mmp1 and Dlp imaging controls at the NMJ terminal.
- Fig. S7. Synaptic Dlp changes with bidirectional *dlp* genetic manipulations.
- Fig. S8. Synaptic Mmp2 changes with bidirectional *dlp* genetic manipulations.
- Fig. S9. Activity-dependent synaptic Dlp increase occurs in the absence of Mmp1.
- Fig. S10. Synaptic Dlp in FXS disease model is restored by single-copy *dlp* coremoval.

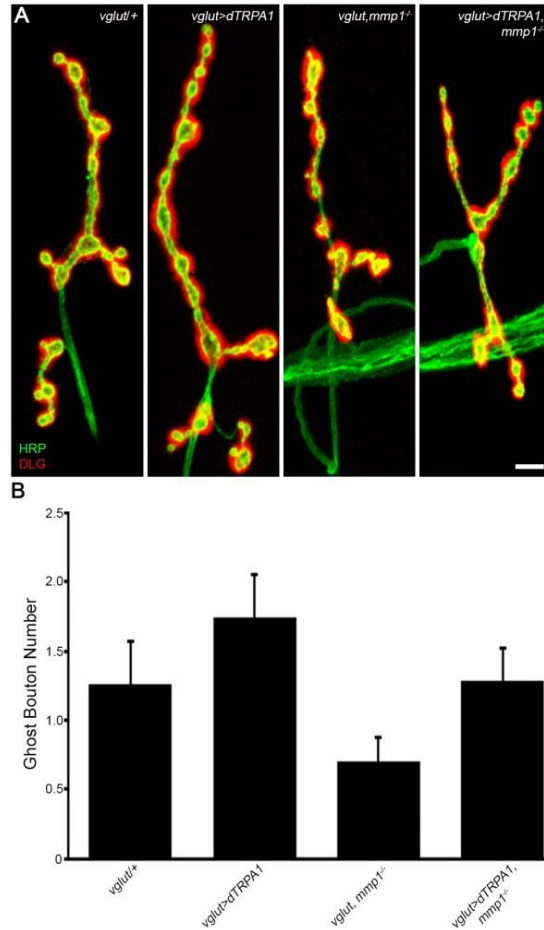


Fig. S1. Temperature controls for dTRPA1 activity-induced synaptic bouton formation. (A) Animals from the 4 genotypes shown were raised at 18°C to the wandering third instar stage, and then the NMJs were co-labeled for presynaptic HRP and postsynaptic DLG. Scale bar: 5 μm. **(B)** Quantification of ghost bouton number: *vglut-Gal4/+* ($n=23$, 1.26 ± 0.31), *vglut-Gal4>UAS-dTRPA1* ($n=35$, 1.74 ± 0.31), *vglut-Gal4,mmp1^{Q112*}/mmp1^{Q112*}* ($n=34$, 0.71 ± 0.17) and *vglut-Gal4>UAS-dTRPA1,mmp1^{Q112*}/mmp1^{Q112*}* ($n=42$, 1.29 ± 0.24). The significance was determined by nonparametric ANOVA (Kruskal-Wallis) and Dunn's multiple comparisons post-test. All comparisons were non-significant ($P>0.05$). Data show mean \pm SEM from at least 3 independent replicates, with n representing the NMJ number.

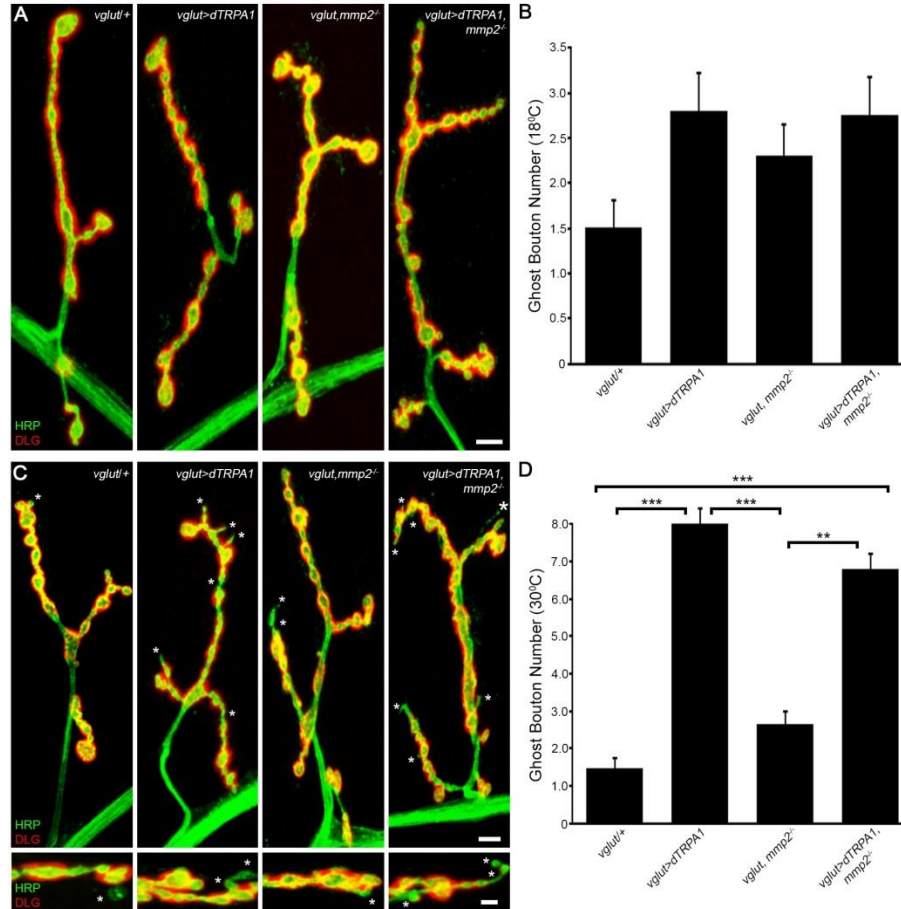


Fig. S2. Mmp2 is not required for activity-dependent synaptic bouton formation. (A and C) NMJs co-labeled for HRP and DLG at 18°C (A) or after dTRPA1 activity stimulation (C) in the 4 genotypes shown. Scale bars: 5 μ m. Higher magnification images of synaptic boutons are shown in (C). Scale bar: 2 μ m. White asterisks mark ghost boutons. **(B)** Quantification of the ghost bouton number at constant 18°C: *vglut-Gal4/+* ($n=29$, 1.52 ± 0.3), *vglut-Gal4>UAS-dTRPA1* ($n=25$, 2.8 ± 0.42), *vglut-Gal4, mmp2^{W307*}/Df(2R)BSC132* ($n=23$, 2.3 ± 0.34) and *vglut-Gal4>UAS-dTRPA1, mmp2^{W307*}/Df(2R)BSC132* ($n=20$, 2.75 ± 0.42). Significance was determined by nonparametric ANOVA (Kruskal-Wallis) and Dunn's multiple comparisons post-test. All comparisons were non-significant ($P>0.05$). **(D)** Quantified ghost bouton number following dTRPA1 activation (1-hour at 30°C): *vglut-Gal4/+* ($n=26$, 1.46 ± 0.31), *vglut-Gal4>UAS-dTRPA1* ($n=28$, 8.0 ± 0.83), *vglut-Gal4, mmp2^{W307*}/Df(2R)BSC132* ($n=26$, 2.65 ± 0.36) and *vglut-Gal4>UAS-dTRPA1, mmp2^{W307*}/Df(2R)BSC132* ($n=24$, 6.79 ± 0.79). Significance was determined by nonparametric ANOVA (Kruskal-Wallis) and Dunn's multiple comparisons post-test, and indicated as *** $P<0.001$ and ** $P<0.01$. Non-significant ($P>0.05$) comparisons 1) *vglut-Gal4/+* vs. *vglut-Gal4, mmp2^{W307*}/Df(2R)BSC132* and 2) *vglut-Gal4>UAS-dTRPA1* vs. *vglut-Gal4>UAS-dTRPA1, mmp2^{W307*}/Df(2R)BSC132* are not shown. Data show mean \pm SEM from at least 3 independent replicates, with n = NMJ number.

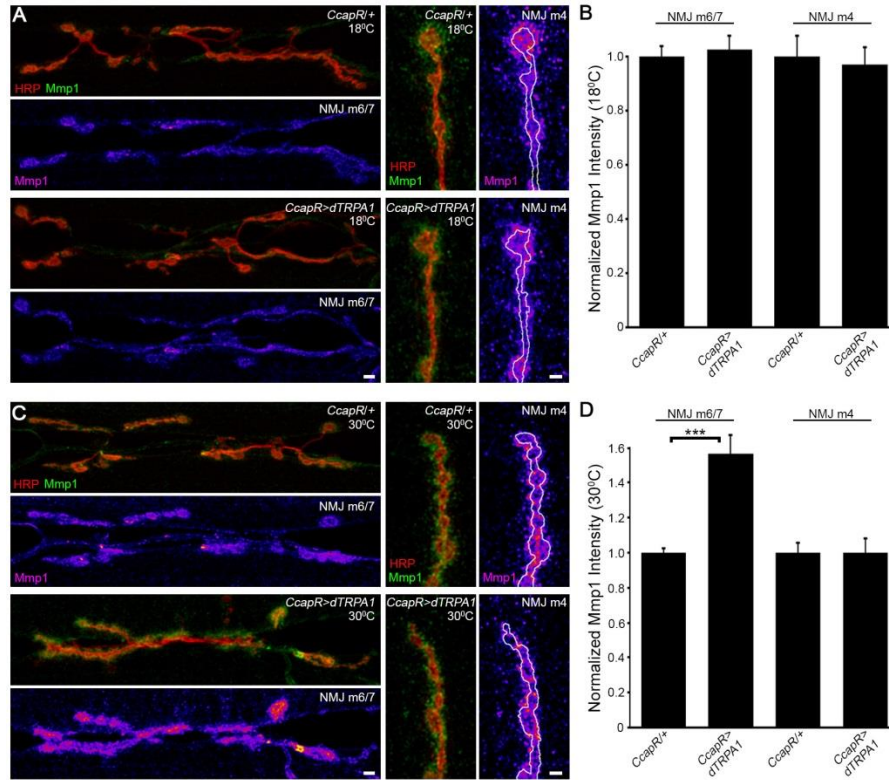


Fig. S3. Mmp1 is rapidly and specifically increased after dTRPA1 neuronal stimulation. (A and C) Images show NMJs co-labeled with HRP and Mmp1 at m6/7 NMJ (scale bar: 5 μ m) and m4 NMJ (scale bar: 2 μ m) in animals reared at dTRPA1-restrictive 18°C (A) or following dTRPA1 stimulation at 30°C for 1 hour (C) in the genotypes indicated. Mmp1 intensity is shown as a heat map. **(B)** Quantification of normalized Mmp1 intensity in the dTRPA1-restrictive condition at m6/7 and m4 NMJs: *CcapR-Gal4*^{+/+} m6/7 NMJ ($n=12$, 1.0 ± 0.04) vs. *CcapR-Gal4*^{>UAS-dTRPA1} m6/7 NMJ ($n=12$, 1.03 ± 0.05) and *CcapR-Gal4*^{+/+} m4 NMJ ($n=16$, 1.0 ± 0.08) vs. *CcapR-Gal4*^{>UAS-dTRPA1} m4 NMJ ($n=14$, 0.97 ± 0.07). Significance determined by Unpaired t-test with Welch correction was non-significant for both ($P>0.05$) and is not shown. **(D)** Quantification of normalized Mmp1 intensity in the dTRPA1-permissive condition at m6/7 and m4 NMJs: *CcapR-Gal4*^{+/+} m6/7 NMJ ($n=16$, 1.0 ± 0.03) vs. *CcapR-Gal4*^{>UAS-dTRPA1} m6/7 NMJ ($n=13$, 1.57 ± 0.1) and *CcapR-Gal4*^{+/+} m4 NMJ ($n=21$, 1.0 ± 0.05) vs. *CcapR-Gal4*^{>UAS-dTRPA1} m4 NMJ ($n=24$, 0.99 ± 0.08). Significance determined by Unpaired t-test with Welch correction (NMJ m6/7), indicated by *** $P<0.001$. Data show mean \pm SEM from at least 3 independent replicates, with n = NMJ number.

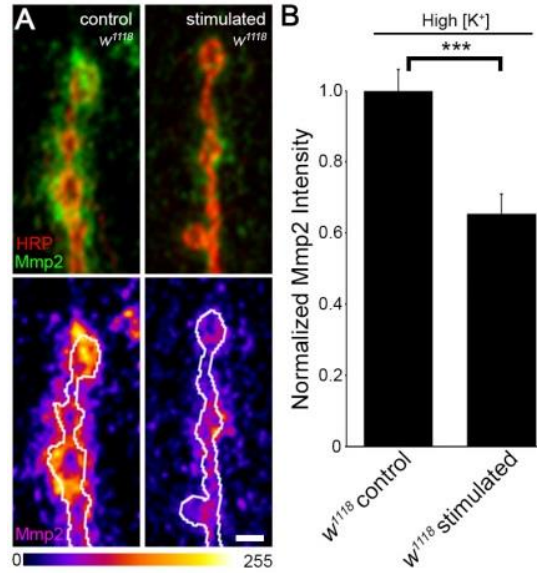


Fig. S4. Synaptic Mmp2 is rapidly reduced after acute neuronal stimulation. (A) Images show NMJs co-labeled for HRP and Mmp2 in either the w^{1118} mock-treated (control) or following 10 minute high $[\text{K}^+]$ stimulation. Heat map shows Mmp2 alone (with intensity scale below) and HRP synaptic outlines in white. Scale bar: 2 μm . (B) Quantification of Mmp2 fluorescent intensity normalized to the unstimulated controls: w^{1118} control (unstimulated, $n=25$, 1.0 ± 0.06) vs. w^{1118} stimulated (high $[\text{K}^+]$, $n=28$, 0.66 ± 0.06). Significance was determined by Unpaired t-test, indicated as *** $P < 0.001$. Data show mean \pm SEM from at least 3 independent experimental replicates, with n = NMJ number.

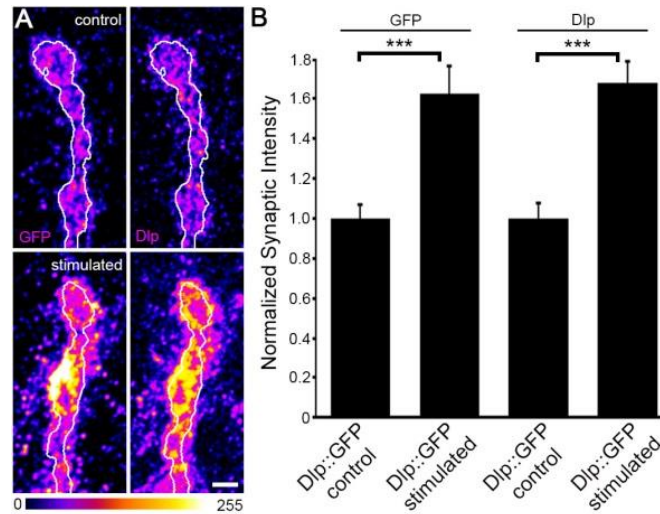


Fig. S5 Synaptic Dlp is rapidly increased after acute neuronal stimulation. (A) Images show NMJs from Dlp::GFP animals co-labeled for GFP and Dlp under standard conditions (control) or following 10 minutes high $[K^+]$ stimulation. Dlp::GFP and Dlp are shown as a heat map (with intensity scale below) and HRP synaptic outlines in white. Scale bar: 2 μ m. (B) Quantification of GFP and Dlp fluorescence intensities normalized to unstimulated controls. GFP: control ($n=24$, 1.0 ± 0.07) vs. stimulated ($n=23$, 1.62 ± 0.14) and Dlp: control ($n=14$, 1.0 ± 0.07) vs. stimulated ($n=15$, 1.68 ± 0.11). Significance was determined by Unpaired t-test with Welch correction, indicated as *** $P < 0.001$. Data show mean \pm SEM from at least 3 independent replicates, with n = NMJ number.

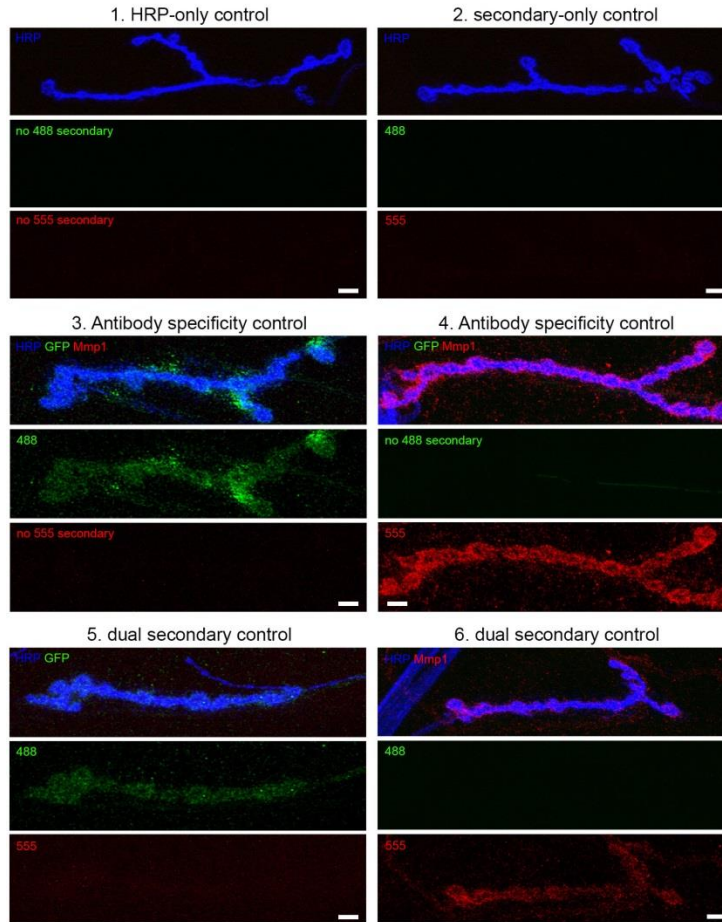


Fig. S6. Synaptic Mmp1 and Dlp imaging controls at the NMJ terminal. Confocal images of Dlp::GFP NMJs labeled with denoted primary (specified in top panels) and secondary antibodies (specified in the middle and bottom panels), processed side-by-side with studies shown in Figure 3. Scale bars: 2 μ m. All conditions included HRP::Cy5 to mark NMJs. Controls included: control 1 terminals labeled with HRP alone; control 2 terminals labeled with HRP and secondary antibodies only (rabbit::488 and mouse::555); control 3 terminals labeled with three primary antibodies (HRP, GFP and Mmp1) but incubated with rabbit::488 secondary only; control 4 terminals labeled with three primary antibodies (HRP, GFP, and Mmp1) and then incubated with mouse::555 secondary only; control 5 terminals labeled with the two primary antibodies (HRP and GFP) and then incubated with the two secondary antibodies (rabbit::488 and mouse::555); and control 6 terminals labeled with two primary antibodies (HRP and Mmp1) and then incubated with the two secondary antibodies (rabbit::488 and mouse::555).

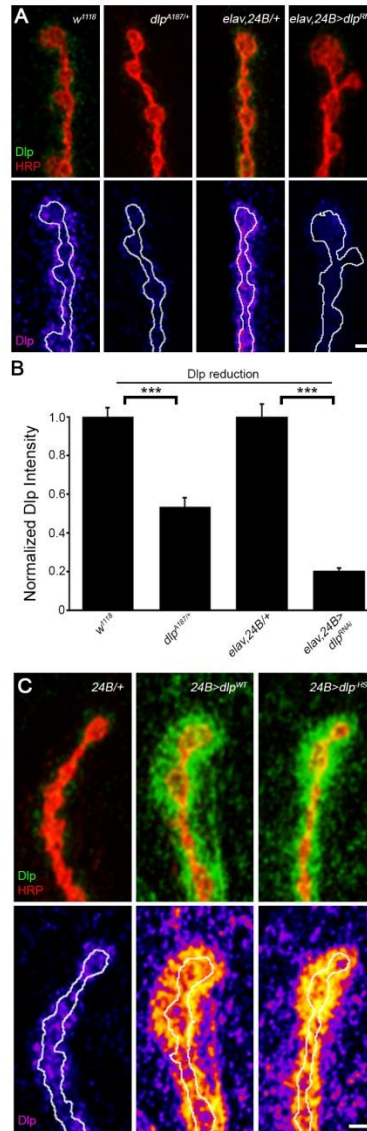


Fig. S7. Synaptic Dlp changes with bidirectional *dlp* genetic manipulations. (A) Images show NMJs co-labeled for HRP and Dlp in the 2 indicated *dlp* reduction conditions compared to matched genetic controls. Dlp is shown in a heat map and HRP synaptic outlines in white. Scale bar: 2 μ m. (B) Quantified Dlp fluorescence intensity normalized to controls: *w¹¹¹⁸* ($n=21$, 1.0 ± 0.04), *dlp^{A187/+}* ($n=23$, 0.54 ± 0.04), *elav-Gal4, 24B-Gal4/+* ($n=9$, 1.0 ± 0.06) and *elav-Gal4, 24B-Gal4>UAS-dlp^{RNAi}* ($n=11$, 0.21 ± 0.01). Significance was determined by Unpaired t-test (*w¹¹¹⁸* vs. *dlp^{A187/+}*) or Unpaired t-test with Welch correction, indicated as *** $P<0.001$. Data show mean \pm SEM from at least 3 independent replicates, with n representing NMJ number. (C) NMJ images co-labeled as in (A) for the 2 indicated *dlp* overexpression conditions compared to transgenic control. Scale bar: 2 μ m. $n=5$ NMJs.

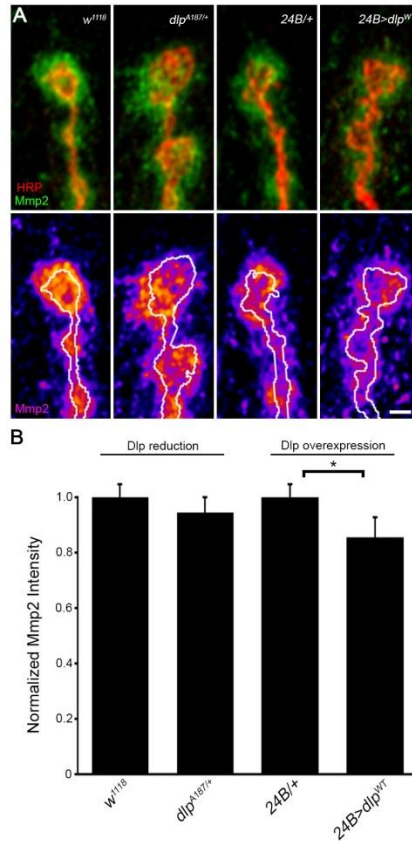


Fig. S8. Synaptic Mmp2 changes with bidirectional *dlp* genetic manipulations. (A) Images show NMJs co-labeled for HRP and Mmp2 in the indicated *dlp* genotypes compared to matched controls. Mmp2 is shown in a heat map and HRP synaptic outlines in white. Scale bar: 2 μ m. (B) Quantification of Mmp2 fluorescence intensity normalized to matched genetic controls: *w¹¹¹⁸* ($n=39$, 1.0 ± 0.05) vs. *dlp^{A187/+}* ($n=44$, 0.94 ± 0.06), and *24B-Gal4/+* driver control ($n=29$, 1.0 ± 0.05) vs. *24B-Gal4>UAS-dlp^{WT}* ($n=31$, 0.86 ± 0.07). Significance determined by Unpaired t-test (*w¹¹¹⁸* vs. *dlp^{A187/+}*) was non-significant ($P>0.05$; not shown). Significance determined by the Mann-Whitney U-Test (*24B-Gal4/+* vs. *24B-Gal4>UAS-dlp^{WT}*) indicated as $*P<0.05$. Data show mean \pm SEM from at least 3 independent replicates, with n = NMJ number. See Figure S7 for Dlp abundance in the genetic manipulations reported here.

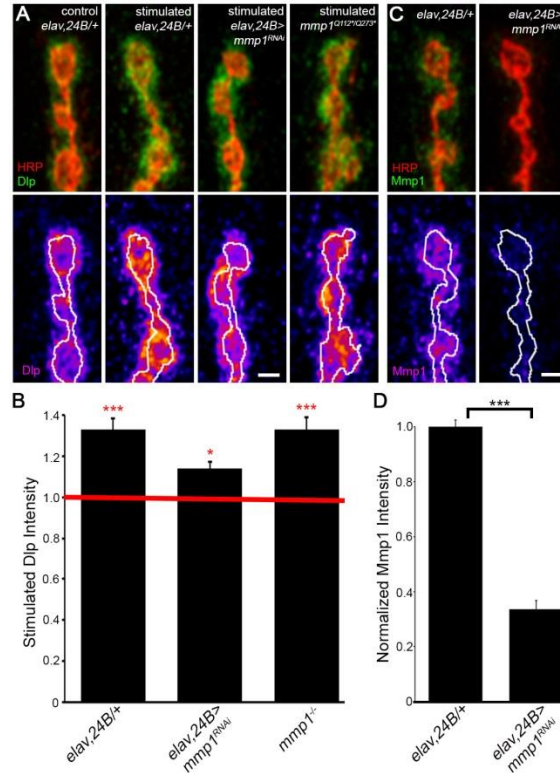


Fig. S9. Activity-dependent synaptic Dlp increase occurs in the absence of Mmp1. (A) Images show NMJs co-labeled for HRP and Dlp in the indicated genotypes, mock treated (unstimulated) or stimulated with high $[K^+]$. Dlp is shown in a heat map and HRP synaptic outlines in white. Scale bar: 2 μ m. (B) Quantification of stimulated Dlp intensity (bar graphs) normalized to unstimulated controls (red line): *elav-Gal4, 24B-Gal4/+* control (unstimulated, $n=14$, 1.0 ± 0.05) vs. stimulated *elav-Gal4, 24B-Gal4/+* ($n=14$, 1.33 ± 0.05), and *elav-Gal4, 24B-Gal4>UAS-mmp1^{RNAi}* (unstimulated, $n=21$, 1.0 ± 0.04) vs. stimulated *elav-Gal4, 24B-Gal4>UAS-mmp1^{RNAi}* ($n=20$, 1.14 ± 0.04) and unstimulated *mmp1^{Q112*/mmp1^{Q273*}}* ($n=22$, 1.0 ± 0.04) vs. stimulated *mmp1^{Q112*/mmp1^{Q273*}}* ($n=25$, 1.33 ± 0.06). (C) Images show NMJs co-labeled for HRP and Mmp1 in the indicated genotypes. Heat map shows Mmp1 alone and HRP synaptic outlines in white. Scale bar: 2 μ m. (D) Quantification of Mmp1 intensity: *elav-Gal4, 24B-Gal4/+* control ($n=18$, 1.0 ± 0.02) and *elav-Gal4, 24B-Gal4>UAS-mmp1^{RNAi}* ($n=21$, 0.34 ± 0.03). (B,D) Significance determined by Unpaired t-test, indicated as * $P < 0.05$ and *** $P < 0.001$. Data show mean \pm SEM from at least 3 independent replicates, with $n =$ NMJ number.

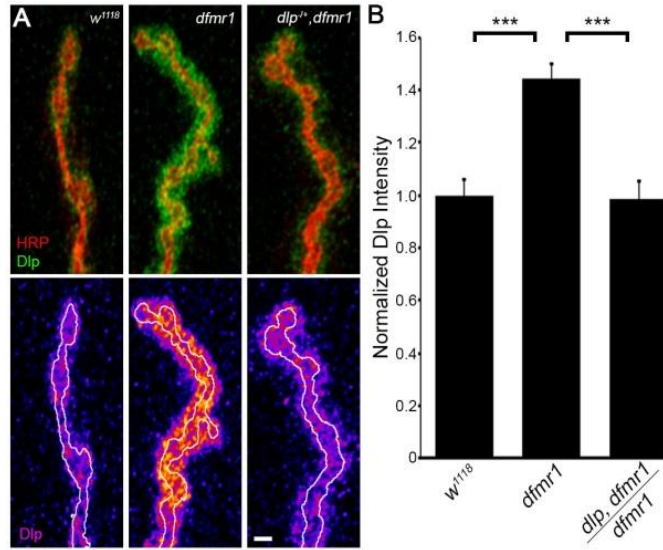


Fig. S10. Synaptic Dlp in FXS disease model is restored by single-copy *dlp* coremoval. (A) Images show NMJs co-labeled for HRP and Dlp in the 3 indicated genotypes. Dlp is shown in a heat map and HRP synaptic outlines in white. Scale bar: 2 μ m. (B) Quantification of normalized Mmp1 fluorescence intensity: *w¹¹¹⁸* control ($n=13$, 1.0 ± 0.06), *dfmr1^{50M/50M}* ($n=16$, 1.44 ± 0.06) and *dlp^{A187/+}, dfmr1^{50M/50M}* ($n=20$, 0.98 ± 0.07). Significance was determined by nonparametric ANOVA (Kruskal-Wallis) and Dunn's multiple comparisons post-test, indicated as *** $P<0.001$. The non-significant ($P>0.05$) comparison for *w¹¹¹⁸* vs. *dlp^{A187/+}, dfmr1^{50M/50M}* is not shown. Data show mean \pm SEM from at least 3 independent replicates, with n = NMJ number.